

# Four dimensions in motivic gravity

M. D. Sheppeard

February 2020

## Abstract

Particle physics is traditionally the study of path integrals for a four dimensional spacetime, where the subtlety is in the existence of smooth structures in dimension 4. From a motivic perspective, however, geometry is interpreted as categorical axioms for quantum computation, and here we bridge the divide between gauge theories and quantum computation by studying the common factor: knot and ribbon diagrams.

## Contents

<b>1</b>	<b>The tower of theories</b>	<b>2</b>
<b>2</b>	<b>Towards 4-manifold invariants</b>	<b>3</b>
2.1	The role of $\mathbf{e}_8$ . . . . .	5
2.2	The Kirby calculus and electric charge . . . . .	7
<b>3</b>	<b>Knots and gravity</b>	<b>7</b>
3.1	Electric magnetic duality and the $j$ -invariant . . . . .	8
3.2	Qutrit rest mass eigenvalues . . . . .	11
<b>4</b>	<b>The categorical view</b>	<b>12</b>
4.1	The pentagon of trees . . . . .	14
4.2	Fibonacci braids and condensation . . . . .	15
4.3	Templates and ribbons . . . . .	19
4.4	Simplices and polytopes . . . . .	20
<b>5</b>	<b>Motivic pairings</b>	<b>23</b>
<b>A</b>	<b>Number Theory</b>	<b>25</b>
A.1	Quadratic fields . . . . .	25
A.2	Fields on cube roots . . . . .	26
A.3	Fields on fourth roots . . . . .	26
A.4	Fields on fifth and higher roots . . . . .	27
A.5	Primes and lattices . . . . .	27
<b>B</b>	<b>Modular tensor categories</b>	<b>28</b>

# 1 The tower of theories

In motivic gravity we study the specialness of four dimensions from a categorical perspective, which is radically different from classical geometry. From this viewpoint [1][2][3], physical axioms for categories become increasingly complex, beyond the knot and ribbon categories [4][5][6] in dimension 3, which underlie topological quantum computation for anyon and gapped boundary systems [7]. We permit additional time directions, since every string in a quantum circuit is permitted to twist about in its time domain, prior to the consideration of a global spacetime. However, in this paper we focus on the usual four dimensions, which follow from the localisation principle of the neutrino CMB correspondence.

In the gauge theory setting, the Jones polynomial for links appears [8] with the Wilson loops for the Chern-Simons action. Inspired by holographic principles, we ask how natural structures in any given low dimension are associated to structures in nearby dimensions. From the motivic perspective, both gauge groups and spacetimes emerge from the laws of quantum computation. In this context, we study Witten's tower of dimensions [9][10] in terms of categorical algebra and number theory. Figure 1 indicates heuristically how vertices in dimension 2 and braids in  $2 + 1$  dimensions are extended to higher dimensions.

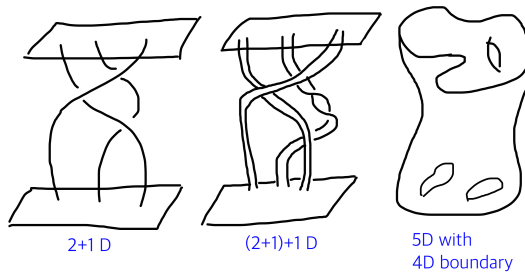


Figure 1: A knotty connection between theories

The Jones invariant [11] is interpreted [9] in 4D using electric magnetic duality, and this is extended to 5D with categorification of the knot polynomials to Khovanov homology [12][13], in a theory on  $X_4 \times \mathbb{R}$  for  $X_4$  a 4-manifold.

For us, electric magnetic duality is associated to the dyonic structure of ribbon particle states, thought of as a double copy of a theory in 3D. In the simplest scheme, diagrams in  $S^3$  acquire a  $U(1)$  fibre to give an  $SU(2) \times U(1)$  compactified Minkowski space, but only as an emergent feature of the discrete  $SU(2)$  braid group representations with integral ribbon twists. Alternatively, a complexification of the Chern-Simons action takes us to a subtle theory in 6 dimensions [10] (associated perhaps to the 10D type IIB theory on  $\mathbb{R}^2 \times \Omega_2^+(X_4) \times \mathbb{R}$  for a 4-manifold  $X_4$ ). Our intuition might start with the Donaldson theory [14] for instanton moduli spaces, but six dimensions appears fundamentally in the computational categories. Moreover, when the gauge group determines space-time, the complexification of the Chern-Simons action immediately suggests a

six dimensional setting. Motivic gravity starts [3] with two copies of CSFT: one for QCD and one for the IR scale of neutrino mass.

Topology change is morally a topos theoretic concept [15]. For exotic structures on 4-manifolds we restrict our attention to integral forms and associated knot and link diagrams [16]. In motivic topos theory, real manifolds and real analysis are not a good starting point for the discussion of emergence. On the contrary, one expects the axioms to merge geometric diagrams with number theory and combinatorics, just as Feynman amplitudes are typically evaluated in a ring of periods rather than  $\mathbb{C}$ .

Our algebras are generically noncommutative and nonassociative. The appendix shows how algebraic number theory is linked to basic observables in quantum mechanics. We insist that observables dictate algebra, in order to minimise the analytical baggage that must be carried around, and beyond that, analysis itself should be re-axiomatised in an  $\infty$ -category that governs quantum logic.

In the computation of scattering amplitudes, it is now well known that the compactification of moduli spaces is combinatorial, starting with the associahedra polytopes [17] for the real points of the Riemann sphere moduli on  $n + 1$  marked points [18], where the associahedron is an axiom for an  $n$ -category. In this paper we explain how algebras associated to the associahedra polytopes are closely related to knots. The Catalan numbers may be deformed by two parameters  $q$  and  $t$ , associated to the double grading in Khovanov homology [19]. A three parameter generalised Jones polynomial has a cyclotomic structure, coming from a natural choice of number field.

The connection between instanton moduli and knots is studied using fermion condensates [20], both for (supersymmetric) QCD and an IR counterpart, which we always attribute to neutrino gravity [3]. The theory utilises extra time dimensions, but localisation to dimension 4 is clearly physically important, and results from the natural selection of one right handed neutrino state in the cosmological CMB correspondence, discovered in 2010 [21][22].

Knots are extended to ribbons, which are the building blocks of template diagrams. All diagrams are interpreted category theoretically, giving us the freedom to start with algebraic integers rather than  $\mathbb{C}$ . Invariants for templates require Hopf algebras and generalisations, starting with 3-manifold invariants from framed links, and the Kirby calculus.

This paper's expository sections are designed to be read in the order given, as we must cover a range of subjects that will not be familiar to all readers. I hope to convince you that the categorical perspective is the correct way to approach axioms for motivic gravity.

## 2 Towards 4-manifold invariants

Experimental precision does not actually require  $\mathbb{R}$  or  $\mathbb{C}$ , except perhaps in axiomatic questions of computability. Like with the adèle numbers, where  $\mathbb{R}$  appears at the infinite prime, we imagine manifolds emerging in ideal, infinite

computations, for which the natural number field is governed by the quantum mechanical questions. Moreover, in moving from the holographic 2 + 1 dimensions into 4D, with ribbons for electric magnetic duality, we naturally work with an emergent Lorentzian metric, because our braid group  $B_3$  will represent  $SU(2)$  in a compactified Minkowski space  $SU(2) \times U(1)$ .

What nice integral ring should we start with? Consider the various triangles in the pentagram of figure 15 (in the appendix). The little blue triangle below the bisected top spike of the pentagram is equivalent to the top blue right angled triangle with an angle of  $18^\circ = \tan^{-1}(\phi\rho)^{-1}$ , where  $\phi = (1 + \sqrt{5})/2$  is the golden ratio and  $\rho = \sqrt{\phi + 2}$  is the diagonal of the golden rectangle. The little  $18^\circ$  bisects the  $36^\circ$  at the red chord, which is a piece of a smaller red pentagon, initiating a zoom-in quasilattice of pentagon coordinates, such that each zoom scales lengths by  $\phi^2$ . In [23] it is shown that the 8 dimensional rational integers  $\mathbb{Z}^8$  may be embedded in  $\mathbb{C}$  using the so called golden ring  $\mathbb{Z}[\rho]$ . One basis in  $\mathbb{R} \subset \mathbb{C}$  is given by (36),

$$x = x_0 + x_1\phi + x_2\rho + x_3\phi\rho. \quad (1)$$

Eight dimensions, in the form  $x + iy$ , is special because of the  $\mathfrak{e}_8$  lattice and its intersection form. Another useful number is  $\sigma = \sqrt{3 - \phi}$ , satisfying  $\rho = \sigma\phi$ . Given any ring, we either work with modules or we have a field of fractions as a base for a category of vector spaces.

Starting with vertex operators, there are four types [24] of Fibonacci ribbon categories, all using golden geometry: two based on minimal models and two for the affine chiral algebras  $G_{2,1}$  and  $F_{4,1}$ . Note that  $G_{2,1} \times F_{4,1} \subset E_{8,1}$ . The affine VOAs correspond to a central charge

$$c = \frac{k \dim(\mathfrak{g})}{k + h^\vee} \quad (2)$$

at level  $k$ , and in general the deformation parameter  $u$  is given by

$$u^{-1} = e^{\pi ic/2}. \quad (3)$$

For  $\phi(u^2 + 1) = -u$ , we have the usual Fibonacci objects  $I$  and  $X$  with the quantum dimension of  $X$  equal to  $\phi$ . The Yang-Lee model at the tenth root  $u = e^{\pi i/5}$  is the representations of the model  $M(2,5)$  with  $c = -22/5$ . In the modular categories, for a unitary VOA, the ribbon twist is given by the conformal weight. The modular matrices here take the form

$$S = \rho^{-1} \begin{pmatrix} 1 & \phi \\ \phi & -1 \end{pmatrix}, \quad T = u^{1/6} \begin{pmatrix} 1 & 0 \\ 0 & u^2 \end{pmatrix}. \quad (4)$$

For  $G_{2,1}$  at  $u = e^{3\pi i/5}$  the phase  $u^{1/6}$  in  $T$  is still golden, and similarly for  $F_{4,1}$ . In other words, the modular matrices contain nice integers. If we wanted a basic deformation of  $\omega = (-1 + \sqrt{-3})/2$  for the Eisenstein integers, we would require  $c = 6$ , which appears in a (4,4) superconformal theory for Mathieu moonshine.

We do not use gauge theory to evaluate knot invariants. The Jones or HOMFLYPT polynomials are evaluated using skein relations, and the Khovanov complex is defined as usual using smoothings. Since our link strands are not geometric in the classical sense, what matters is the information content, or complexity, of a diagram.

## 2.1 The role of $\mathbf{e}_8$

A 4-manifold is characterised by its integral form [16], and a key component of the classification of integral forms is the  $\mathbf{e}_8$  form

$$E_8 = \begin{pmatrix} 2 & 1 & 0 & 0 & 0 & 0 & 0 & 0 \\ 1 & 2 & 1 & 0 & 0 & 0 & 0 & 0 \\ 0 & 1 & 2 & 1 & 0 & 0 & 0 & 0 \\ 0 & 0 & 1 & 2 & 1 & 0 & 0 & 0 \\ 0 & 0 & 0 & 1 & 2 & 1 & 0 & 1 \\ 0 & 0 & 0 & 0 & 1 & 2 & 1 & 0 \\ 0 & 0 & 0 & 0 & 0 & 1 & 2 & 0 \\ 0 & 0 & 0 & 0 & 1 & 0 & 0 & 2 \end{pmatrix}. \quad (5)$$

But an  $\mathbf{e}_8$  manifold cannot be smooth, because the form does not diagonalise over the rational integers. It does however diagonalise [25] over the golden integers  $\mathbb{Z}[\phi]$ , where  $\phi = (1 + \sqrt{5})/2$  is the golden ratio. As is well known,  $E_8$  is positive definite, even and unimodular. Let  $\sigma(Q)$  be the signature of the form  $Q$  and  $r(Q)$  its rank. All such quadratic forms take the form [16]

$$Q = \frac{\sigma(Q)}{8} E_8 \oplus \frac{r(Q) - |\sigma(Q)|}{2} \begin{pmatrix} 0 & 1 \\ 1 & 0 \end{pmatrix}, \quad (6)$$

where the  $2 \times 2$  factors are forms for either the torus  $T^2$  (for  $H_1(T^2, \mathbb{Z}_2)$ ) or  $S^2 \times S^2$  in dimension 4. This ambiguity will matter later on.

One important smooth space, which contains a topological component that cannot be smoothed, is the Kummer (or K3) surface, with its 22 dimensional form

$$Q_{K3} = E_8 \oplus E_8 \oplus \begin{pmatrix} 0 & 1 \\ 1 & 0 \end{pmatrix} \oplus \begin{pmatrix} 0 & 1 \\ 1 & 0 \end{pmatrix} \oplus \begin{pmatrix} 0 & 1 \\ 1 & 0 \end{pmatrix}. \quad (7)$$

The construction uses a connected sum of three copies of the 4-manifold  $S^2 \times S^2$ , corresponding to the triple of flip matrices. A quotient of this sum by a certain embedding, related to the Kummer surface, yields a fake version of  $\mathbb{R}^4$ , and a theorem of Freedman [26] characterises so-called good copies of  $\mathbb{R}^4$  by the conditions: simply connected, non-compact, without boundary,  $H_2(M, \mathbb{Z}) = 0$ , an end homeomorphic to  $S^3 \times [0, \infty)$ . It turns out that there are an uncountable number of inequivalent smooth structures on  $\mathbb{R}^4$ , and this complexity is unique to dimension 4 due to surface knotting. One class of exotic  $\mathbb{R}^4$  are called *ribbon*, and these are diffeomorphic to open subsets of ordinary  $\mathbb{R}^4$  [16].

The elliptic genus for the K3 surface [27] is

$$Z_{K3}(\tau, z) = 8\left[\left(\frac{\theta_2(\tau, z)}{\theta_2(\tau, 0)}\right)^2 + \left(\frac{\theta_3(\tau, z)}{\theta_3(\tau, 0)}\right)^2 + \left(\frac{\theta_4(\tau, z)}{\theta_4(\tau, 0)}\right)^2\right], \quad (8)$$

for  $\theta_i(\tau, z)$  the Jacobi theta functions. Nowadays it is written in terms of dimensions of irreducible representations [28] for the Mathieu group  $M_{24}$ , in Mathieu moonshine [29] and its umbral generalisation [30]. Moonshine for the Monster group uses the  $j$ -invariant, which is analogously defined by

$$j(q) = 32 \frac{(\theta_2(0, q)^8 + \theta_3(0, q)^8 + \theta_4(0, q)^8)^3}{(\theta_2(0, q)\theta_3(0, q)\theta_4(0, q))^8}. \quad (9)$$

The associated Eisenstein series  $E_4$  counts vectors in the shells of the  $\mathbf{e}_8$  root lattice. These discrete lattices underlying modular forms are fundamental, just as combinatorial polytopes capture computations in scattering theory. In fact, the associahedra polytopes sit naturally inside certain cubic lattices.

Rather than plain  $\mathbb{Z}^8$ , it will be natural to use integral octonions to define the  $\mathbf{e}_8$  lattice. That is, we introduce noncommutative and nonassociative rings for the study of 4-manifolds.

Whenever we see a triplet of terms, as in (9), we think of some form of triality. In the Jordan algebra  $J_3(\mathbb{O})$ , triality acts on the three off diagonal copies of  $\mathbb{O}$ , and this extends to generalised  $3 \times 3$  algebras for ribbon categories, which have higher dimensional matrix entries.

What about the physics? The exact gauge symmetries  $U(1)_Q$  and color  $SU(3)_C$  are directly associated, respectively, to ribbon twists and a triplet of ribbon strands, so that the 8 negative electric charges for  $\{\nu, e^-, d, \bar{u}\}$  lie on the vertices of a 3-cube [31][32], whose directions label ribbon strands. Such a 3-cube, in figure 2, determines a basis for the octonions  $\mathbb{O}$ . Complexification brings in antiparticles, for a total 4-cube of charges, and complex conjugation is charge conjugation in the  $\mathbb{C} \otimes \mathbb{O}$  ideal algebra, which extends to crossing flips in the ribbon picture. A 7-cube introduces magnetic data with seven stranded ribbon diagrams, and in general, the extended M theory dimension equals twice the number of ribbon strands.

The electroweak symmetries are broken back-to-front: the Higgs mass emerges from the inverse see-saw rule [3], which pairs the Planck scale and IR neutrino mass scale at 0.01 eV, and chirality also appears explicitly in the ribbon diagrams. There is no need to introduce further local states beyond the SM, because the new RH neutrino is associated to a cosmological scale, and we are already sure that the theory is not Lagrangian.

Now as a higher gauge symmetry, we will see that  $\mathbf{e}_8$  itself emerges from the axioms for quantum computation, through the Hopf algebras that define ribbon invariants. The same holds for lattices in higher dimensions, which are associated to more general ribbon algebras.

## 2.2 The Kirby calculus and electric charge

An axiomatic approach to invariants constructs state sums from categorical data. Barrett et al [33] consider a functor from a spherical fusion category into a ribbon fusion category for the 2-handlebody of the 4-manifold, in order to define smooth invariants by weakening the sliding law in a ribbon category. A 4-manifold is determined up to diffeomorphism by its 2-handlebody attachments, where a 2-handle piece is essentially a framed knot in the  $S^3$  boundary of the 0-handle.

For a 2-handle in 4 dimensions, the framing classes are characterised by  $\pi_1(O(2)) = \mathbb{Z}$  [16], whereas in 3 dimensions the only framings are 1 or  $\theta^{1/2}$ , where  $\theta$  represents a full ribbon twist. This distinction is crucial to us, because quantised electric charge is given by ribbon twists. Three dimensions only permits two charges, whereas physics requires three values  $0, \pm 1$ . Often we denote these charges [1] by the cubed roots of unity 1,  $\omega$  and  $\bar{\omega}$ , when  $\theta$  behaves like a phase. To obtain  $\mathbb{Z}_3$  we have to go to four dimensions, and quotient out by the natural  $3\mathbb{Z}$  that appears: a triple of half twists  $\theta^{3/2}$  equals  $-1$  under the cubed root representation, while  $B_2 = \mathbb{Z}$  represents  $-1$  by a single half twist. In other words, charge appears only with the holographic extension of  $2 + 1$  dimensions to four.

A Kirby diagram [34] of knots and balls accounts for all the attachments in  $\mathbb{R}^3$  for a 4-manifold (there are really no real numbers, just diagrams). A single knot in the Kirby diagram will cancel a 1-handle (two balls in  $\mathbb{R}^3$ ) if it has ends attached to each ball. In an Akbulut diagram, the balls of a 1-handle are replaced by marked circles, so that the entire 4-manifold is specified by a diagram for a ribbon fusion category [6].

We are interested in modular ribbon categories (see appendix B), which have a finite number of isomorphism classes of simple objects and an invertible matrix  $s_{ij}$  defined by Hopf links on the objects  $i$  and  $j$ . In section 4.3, Kirby framed link diagrams are associated to ribbon vertices, and we see how simple ribbon pictures may give rise to complicated links.

## 3 Knots and gravity

Sections 4 and 5 discuss further the categorical interpretation of link diagrams. In this section we discuss the physical justification for this approach. Categorical axioms lie nowadays at the foundation of both condensed matter physics and computer science. It turns out that topological insulators, for instance, are a good intuition for the dyonic mirror [35] that defines holography in the ribbon particle scheme.

At its simplest, quantum mechanics is about finite fields and complex numbers. Beyond  $\mathbb{C}$  we strike the noncommutative quaternions  $\mathbb{H}$  in four dimensions and then the nonassociative octonions  $\mathbb{O}$  in eight dimensions. In any dimension, we start with an integer lattice. For  $\mathbb{H}$ , the three Pauli generators are called  $I, J$  and  $K = IJ$ . In the octonions  $\mathbb{O}$ , we do not assume that  $K$  belongs to

Table 1: Arrow dimensions for ribbon pair

dim	0	1	2	3	4
$\mathcal{C}$	•	•	ob	ar	axiom
$\mathcal{C}^\vee$	axiom	ar	ob	•	•

a quaternion triplet. Then the 8 basis units of  $\mathbb{O}$  are conveniently given by figure 2, which considers various subsets and intersections of the three point set  $\{I, J, K\}$ .

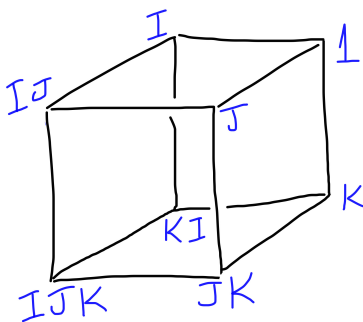


Figure 2: Octonion units on a cube

Every diagram is interpreted categorically, so that a cube exists in the same sense as an associahedron, which appears as an axiom for an  $n$ -category. On the one hand we have these discrete spaces, and dually we have generalised string diagrams. Three dimensions occurs in nature precisely because of the utility of 3 dimensional structures. Thus four geometric dimensions correspond to a 4 dimensional category, where braid diagrams usually define arrows in dimensions 2 and 3, just as the structure of a 4-manifold comes down to diagrams in dimension 3. The emphasis is different from 4-categories for geometric quantisation based on symmetry [36], but we still have to consider arrows in dimensions 0 and 1 (which are trivial for a braided monoidal category) and the idea is to associate geometric duality to cohomological duality, where the second ribbon category occupies the dual dimensions, as shown in Table 1. Dimension 4 is the only time that objects coincide.

### 3.1 Electric magnetic duality and the $j$ -invariant

A half unknot, with trivial framing in the Kirby calculus, is a wormhole pair creation diagram for entanglement [37]. The basic electric charges of the (massless) Standard Model are listed in Table 2, as ribbon diagrams on three strands, built from Dirac strings. The mirror set of diagrams introduces the extra magnetic degrees of freedom, so that particles on either side of the mirror carry dyonic charge (see section 4.2). Observe that all neutrino helicities occur, but there are



no additional local particle states beyond the SM.

The Chern-Simons action is applied to gravity in 2 + 1 dimensions, via the Monster CFT [38] of central charge 24. In motivic gravity, this theory builds the mass gap for neutrinos, which underpin the Higgs mechanism, and there is a second CSFT for QCD and the strong CP problem. The partition function of [38] is the modular  $j$ -invariant for elliptic curves. Recall that this invariant is defined in terms of the Eisenstein forms  $E_4$  and  $E_6$ , where  $E_4$  counts roots on the  $\mathbf{e}_8$  lattice. The  $j$ -invariant itself counts irreps for the Monster moonshine module, associated to the symmetries of the Leech lattice.

The relation between the  $j$ -invariant and the golden ratio  $\phi = (1 + \sqrt{5})/2$  is explained in [39]. Compare the factor of 32 in (9) with the common normalisation of  $1728 = 64 \times 27$ . The  $2048 = 64 \times 32$  equals  $j(\pm\phi)$ , and the set  $\{\pm\phi, \pm\phi^{-1}\}$  is included in a critical set of real values of  $j$ . Note that the conjugates of  $\phi$  solve the quadratic in  $x$  which results from insisting on (i) the geometric sequence  $F_{n+1} = xF_n$  and (ii) the Fibonacci recursion  $F_{n+2} = F_{n+1} + F_n$ . Thus  $\phi = 2 \cos \pi/5$  is a placeholder for all the rationals  $F_{n+1}/F_n$ .

The bosonic braid states are defined using the discrete Fourier transform of Table 2, resulting in 6 neutral mixed states on top of the diagonal  $W^\pm$  and  $\gamma$  diagrams, from which to build a  $Z$  boson. Combined with spinor information, this gives our 24 dimensional internal space, starting with the Leech lattice [40][41]. Each point of the  $\mathbf{e}_8$  lattice is surrounded by 2160 orthoplexes and  $17280 = 8 \times 2160$  simplices.

To understand duality, we need to look at combinatorial degrees of freedom [1]. Two copies of the group  $\mathbf{e}_8$  have a total of 480 root directions, in

$$496 = 2(28 + 28) + 2(8 \times 8 + 8 \times 8 + 8 \times 8) \quad (10)$$

dimensions, giving 8 copies of 14 in the adjoint part. These are our *basis associahedra*. The octonion factors of 8 will be associated to 3-cubes, so that everything is encoded in dimension 4. More conventionally, the 14 trees denote a 14 dimensional theory associated to the 3-time grading [42]

$$\mathbf{e}_{8(-24)} = 14 + 64 + (SO(11, 3) + 1) + 64 + 14. \quad (11)$$

Here the  $64 = 35 + 21 + 7 + 1$  counts the ordered subsets of up to three distinct units in  $e_1, \dots, e_7$ , and another 64 counts the subsets of size  $\geq 4$ . That is, we have a 3-brane and magnetic 7-brane and the usual  $SO(9, 1) \simeq SL_2(\mathbb{O})$  embeds in  $SO(11, 3)$ . As noted, for us 7 dimensions means 7 ribbon strands, for a total of 14 braid strings, all in dimension 3. One may extend [42] the above to a (7, 11) pair of branes in a (19, 3) theory, in the tower of exceptional periodicity. Eventually we find  $SO(28, 4)$ , breaking to  $SO(3, 3) \times SO(25, 1)$ , where the 32 dimensions is high enough to obtain four copies of the integers  $\mathbb{Z}^8$  to define  $SL_2(\mathbb{C})$ .

In dimension 4, there is a  $1680 = 14 \times 120$  vertex analog of the 120 vertex polytope in figure 12, which itself is a three dimensional representation of  $S_5$ . Two copies of this 120 vertex polytope catalog the roots of  $\mathbf{e}_8$ , so we have 7 copies of  $\mathbf{e}_8$  in the 1680 vertices. This is not excessive, because we actually

want three copies of the Leech lattice in 72 dimensions, based on 9 copies of  $\mathbf{e}_8$ , providing enough integral octonions for three copies of a dense set in  $SL_2(\mathbb{C})$ . This 1680 vertex polytope is an axiom [43] for a categorified modular category.

Note that all higher dimensional associahedra are products of the polytopes in dimension 2 and 3. The 3 dimensional associahedron is a model for the sheaf cohomology of  $\mathbb{R}P^2$ . As is well known, the associahedra also describe the compactification of the genus zero moduli spaces  $\mathcal{M}_{0,n}$  of Riemann spheres. At the other extreme, the high genus moduli  $\mathcal{M}_{\infty,1}$  has a completion  $\mathcal{M}_{\infty,1}^+$  [44] such that

$$\pi_3(\mathcal{M}_{\infty,1}^+) = \mathbb{Z}_{24} + G, \tag{12}$$

for some  $G$ , which we assume is related to the stable group  $\pi_{n+3}(S^n) = \mathbb{Z}_{24}$  when  $n \geq 5$ . Baez [44] describes  $\mathbb{Z}$  as the decategorification of a category of tangles, where the objects are strings of  $n \pm$  signs. Recall that 24 signs is the setting of the Golay code, underlying the Leech lattice. Signs for tangles exist whenever duals are present, which is the case for all our categories.

Below we will connect braid group generators directly to the vertices of an associahedron. But there is another deep connection between links and the associahedra, as follows. Given any pair of rooted, binary trees  $t_1$  and  $t_2$  on  $d$  leaves, there is a pairing  $h(t_1, t_2)$  which defines an element of Thompson's  $F$  group [45][46]. A traced pairing diagram built from  $t_1$  and  $t_2$  is a trivalent planar graph, whose edges may be colored with 3 colors such that each vertex carries one edge of each color. A  $\pm$  sign is then attached to each vertex, depending on whether the permutation of (123) is odd or even. The sign determines a link crossing when a trivalent vertex is extended to a crossing piece [46], as in figure 3. It turns out that *all links* may be obtained this way.

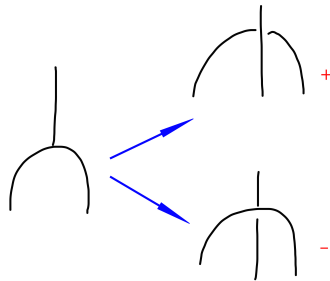


Figure 3: Trivalent vertex maps to link crossing

The four color theorem for planar maps is closely related to these questions, and the connection between this theorem and pentagons has a very long history. We show a 3-coloring of an associahedron in figure 13. One could be forgiven for thinking that the associahedra will solve many outstanding conjectures!

### 3.2 Qutrit rest mass eigenvalues

A *loop* is a quasigroup with an identity, in analogy to a category with a nonassociative product and noncommutative braiding. For example, the integral octonions form a finite nonassociative loop. Product tables for finite loops are Latin squares. Two simple examples of order 3 are the left unit loop and the idempotent loop,

$$L_{lu} = \begin{pmatrix} 1 & a & b \\ b & 1 & a \\ a & b & 1 \end{pmatrix}, \quad L_I = \begin{pmatrix} 1 & b & a \\ b & a & 1 \\ a & 1 & b \end{pmatrix}, \quad (13)$$

which are 1-circulant and 2-circulant symmetric, respectively. In general, an order 3 table is selected [47] from 9 points in the Hamming graph  $H(3, 3)$ , which is the 27 points on the qutrit 3-cube (see section 4.1). For example, the pure state 221 puts a 1 in the second row and second column of  $L_{lu}$ .

Hermitian  $3 \times 3$  matrices in a generalised Jordan algebra are the natural place for rest mass triplets in a low energy regime. They are necessarily 1-circulants, belonging to a group algebra  $\mathbb{F}S_3$  on the three object permutations, and diagonalised over  $\mathbb{C}$  by the quantum Fourier transform (15).

A vector  $(t, x, y, z)$  in Minkowski spacetime is written as a  $2 \times 2$  complex quaternion matrix

$$\begin{pmatrix} t + z & x + iy \\ x - iy & t - z \end{pmatrix}, \quad (14)$$

with the determinant  $t^2 - x^2 - y^2 - z^2$  giving the metric. The corresponding twistor space is the projective space  $\mathbb{CP}^3$ , but we can use a golden ring  $R$  in place of  $\mathbb{C}$ . Because coordinates should be projective,  $R\mathbb{P}^3$  is defined using 4-vectors, interpreted as a double spinor. If  $R$  is eight dimensional over  $\mathbb{Z}$ , as above, then our projective space is secretly a 24 dimensional space. We therefore expect to encounter fundamental phases like  $\pi/4$  and  $\pi/6$  [3]. These phases appear automatically in mutually unbiased bases [48][49][50] for qubits and qutrits. In a prime power dimension  $d = p^r$  there are  $d + 1$  MUBs and  $d - 1$  mutually orthogonal Latin squares, like the pair above for  $d = 3$ . More general Gauss sums for modular categories appear in [51].

Let  $\omega = (-1 + \sqrt{-3})/2$ . The qutrit Fourier transform is given, up to permutations, by

$$F_3 = \frac{1}{\sqrt{3}} \begin{pmatrix} 1 & 1 & 1 \\ 1 & \omega & \bar{\omega} \\ 1 & \bar{\omega} & \omega \end{pmatrix}. \quad (15)$$

Its columns form one basis in a set of four MUBs for qutrits. The other 3 bases form a cyclic group  $C_3 \subset S_3$ , and a cyclic group  $C_d$  appears in any prime power dimension  $d = p^r$  [50]. The density matrices of these columns are the idempotents

$$B = \frac{1}{3} \begin{pmatrix} 1 & \omega & \bar{\omega} \\ \bar{\omega} & 1 & \omega \\ \omega & \bar{\omega} & 1 \end{pmatrix}, \quad C = \frac{1}{3} \begin{pmatrix} 1 & \bar{\omega} & \omega \\ \omega & 1 & \bar{\omega} \\ \bar{\omega} & \omega & 1 \end{pmatrix}, \quad A = \frac{1}{3} \begin{pmatrix} 1 & 1 & 1 \\ 1 & 1 & 1 \\ 1 & 1 & 1 \end{pmatrix}, \quad (16)$$

and a Hermitian mass operator is a combination of these idempotents. Let

$$\sqrt{M} = aA + bB + cC \tag{17}$$

for  $a, b, c$  real. Our masses are the squares of the three eigenvalues of  $\sqrt{M}$ , accounting for the chiral components of our mass states. Without loss of generality, fix a mass scale by the rule  $(a + b + c)^2 = 1$ . The Koide rule [52][53] follows from the eigenvalues of the charged lepton matrix

$$\sqrt{M} = \frac{\sqrt{\mu}}{\sqrt{2}} \begin{pmatrix} \sqrt{2} & \theta & \bar{\theta} \\ \bar{\theta} & \sqrt{2} & \theta \\ \theta & \bar{\theta} & \sqrt{2} \end{pmatrix}, \tag{18}$$

where the scale  $\mu = 4/3$  follows from  $(a + b + c) = 1$ . For charged leptons, the 4 in  $\mu$  rescales to the mass of the proton, and the observed value of  $\theta$  is close to  $2/9$ . The quarks have mass matrices whose phases are  $1/3$  and  $2/3$  of this value. The neutrino scale is around 0.01 eV, and its phases are  $2/9 \pm \pi/12$  [54]. Putting all leptons and quarks (of negative charge) onto a three dimensional cube, we have an effectively 24 dimensional state space, with one quirit for rest mass.

We embed our Hermitian elements of  $J_3(\mathbb{C})$  in a higher dimensional exceptional Jordan algebra [3]. The  $2/9$  Koide parameter is associated to the charge  $U(1)$  in the  $\mathbb{C} \otimes \mathbb{O}$  algebras, so that we can start with the fundamental  $\pm\pi/12$  neutrino phases in  $J_3(\mathbb{C}) \subset J_3(\mathbb{O})$ . Recall that triality acts on the three off-diagonal copies of  $\mathbb{O}$  in a  $3 \times 3$  element of this algebra, and all circulants belong to a group algebra for the permutations  $S_3$ , which is our basic Hopf algebra [55]. Mass matrices use the cyclic group  $C_3 \subset S_3$ , and diagonal mass triplets are functions on  $C_3$ , so that under the Fourier transform the quantum double  $D(S_3)$  of  $S_3$  looks like an algebra  $\mathbb{F}C_3 \otimes \mathbb{F}C_3$ , in which electric magnetic duality will become completely transparent.

The  $B_3$  braid states for the massless SM are given in Table 2. The unlisted mirror braids give the additional magnetic degrees of freedom. Observe how the braiding characterises left and right handed neutrinos, which both contribute to the gravity see-saw [3]. Left and right modes at defects in CFT categories are separated by a braiding [56]. With the given crossings, the product  $(231) = (312)(312)$  is the figure 8 braid, while the mirror  $(312)(312)^m$  is an unknot.

The Fibonacci  $B_3$  representation is  $2 \times 2$ , fitting in three ways into our generic  $3 \times 3$  matrices. A circulant mixing factor is automatically in  $SU(2) \times U(1)$ , and the product of  $F_3$  and the real form of the tribimaximal matrix gives a  $3 \times 3$  representation [54] of the arithmetic phase  $\pi/12$ , which we imagine coming from dimension 72.

## 4 The categorical view

Axiomatically, quantum gravity is about categorical logic for propositions involving the quantum vacuum, whose structure begins with the cosmological

Table 2: Standard Model electric braid states

$\nu_L$ $\sigma_1\sigma_2^{-1}$	$e_L^-$	$\bar{u}_L(1)$	$\bar{u}_L(2)$	$\bar{u}_L(3)$	$d_L(1)$	$d_L(2)$	$d_L(3)$
	---	0--	-0-	--0	-00	0-0	00-
$\bar{\nu}_R$ $\sigma_2\sigma_1^{-1}$	$e_R^+$	$u_R(1)$	$u_R(2)$	$u_R(3)$	$\bar{d}_R(1)$	$\bar{d}_R(2)$	$\bar{d}_R(3)$
	+++	0++	+0+	++0	+00	0+0	00+
$\bar{\nu}_L$ $\sigma_1^{-1}\sigma_2$	$e_L^+$	$u_L(1)$	$u_L(2)$	$u_L(3)$	$\bar{d}_L(1)$	$\bar{d}_L(2)$	$\bar{d}_L(3)$
	+++	0++	+0+	++0	+00	0+0	00+
$\nu_R$ $\sigma_2^{-1}\sigma_1$	$e_R^-$	$\bar{u}_R(1)$	$\bar{u}_R(2)$	$\bar{u}_R(3)$	$d_R(1)$	$d_R(2)$	$d_R(3)$
	---	0--	-0-	--0	-00	0-0	00-

neutrino ansatz [1][3]. Recall that classical logic in physics employs sets and distributive lattices, where Stone's theorem [57] states that the space associated to a lattice is Hausdorff if and only if the lattice is Boolean, defining a category of Stone spaces, which is a special limit of the category of finite sets. Ordered Stone spaces are essentially *coherent* spaces, and coherent locales are essentially locales of ideals in a distributive lattice. Distributive lattices are Boolean only if all prime ideals are maximal. In other words, classical spaces are derived from lattice algebras with a number theoretic flavour.

Quantum mechanics immediately requires nondistributive lattices, and axioms for higher dimensional categories [58]. The combinatorics of quantum field theory [58] associates particle number with dimension, naturally introducing infinite dimensional categories, starting with the 1-operad of the associahedra. The category of Hilbert spaces for quantum mechanics is a symmetric monoidal category, but for gravity we permit a non trivial braiding. All our diagrams are interpreted in this context, where the only proper classical spaces are sets of points.

Replacing the Boolean truth values  $\{0, 1\}$  with  $\mathbb{R}$  takes us from Stone duality to either Gelfand duality (for commutative rings) or  $\mathbb{R}/\mathbb{Z} = S^1$  in Pontryagin duality. But we need not give  $S^1$  a real structure immediately, when algebraic number fields are in play, so long as we note that  $S^1$  should contain a copy of every cyclic group. Quantum mechanical propositions localise to definite rational prime powers, like  $p = 2^2$  for two qubits. Only a maximal category of all possible state spaces, in infinite dimensions, would require a notion of real number. Thus our braid loops, and other strings, are not at all  $S^1$  spaces in the usual sense.

Such obtuseness is entirely justified by the successful application of operads to scattering amplitudes. For nonperturbative structures, we need a monadic connection between algebra and geometry, defining endofunctors on true categories of motives. If a ring  $R$  is commutative, its set of idempotents forms a Boolean algebra, and any commutative  $R$  is a ring of global sections for a sheaf on a Stone space [57]. The canonical such sheaf is the *Pierce sheaf*, based on the Stone space  $\text{spec } I(R)$ , where  $I(R)$  are the idempotents of  $R$ .

Pierce decompositions extend to noncommutative and nonassociative algebras based on  $\mathbb{H}$  and  $\mathbb{O}$ . In particular, the integral part of the exceptional

Jordan algebra  $J_3(\mathbb{O})$  plays a key role in motivic gravity [3][59][60][42]. This setting is categorically deeper than initial forms of noncommutative geometry, which traditionally take fields such as  $\mathbb{R}$  or  $\mathbb{C}$  for granted.

Nondistributive lattices in ordinary quantum mechanics are usually commutative, because for vector spaces the unions  $V \wedge W$  are commutative. Tensor products are also weakly commutative in the symmetric monoidal structure, just as Cartesian products are for sets. Our braidings break this symmetry, and this braiding will characterise the particle spectrum of the Standard Model.

From this categorical perspective, functorial structures, such as adjunctions for mirror symmetry, are completely natural, and appear prior to the usual setting of path integrals on classical spaces. Thus the physical intuition of the bounding of free states is analogous to the creation of algebras with relations from free algebras, where quotients are determined by abstract ideals.

## 4.1 The pentagon of trees

A finite dimensional module over a ring  $R$  typically has a basis set. For example, figure 2 is the lattice of subsets for a three element set  $\{I, J, K\}$ , which form a basis for three dimensional space. Alternatively, any state space for  $n$  qubits defines such a cube, with the vertices the  $2^n$  pure states. Here we have reduced the 8 dimensions of  $\mathbb{O}$  to a 3 dimensional object, whose seven non trivial units give the Fano plane. Similarly, 27 points on a cube with three points along each edge list the pure states for 3 qutrits. Given a three element set  $\{I, J, K\}$ , its subsets are generated by the polynomial

$$(x + I)(x + J)(x + K), \tag{19}$$

and similarly for any  $n$  point set. Setting  $I = J = K = 1$  recovers the binomial coefficients, which generalise to the Gaussian polynomials when  $I = 1$ ,  $J = t^2$ ,  $K = t^{-2}$ . For four variables, the Gaussian polynomials come from  $\{t^{-3}, t^{-1}, t, t^3\}$ , and so on. Thus polynomials in more variables may be obtained when  $I, J$  and  $K$  are not fixed in the usual fashion.

For quantum logic, elements are initially lines, rather than points. In figure 4, we replace words by line configurations. Each letter represents an intersection point, so if we look at the intersection points on the lines, the double letters ( $IJ$  etc.) disappear from the cube, leaving a 5-cell of five points.

A planar projection of a 5-cell is a pentagon. The pentagon of figure 5 carries a variety of labellings. As the first polytope in the sequence of associahedra, it's vertices are the binary rooted trees with five leaves (including the root). The noncommutative forests are easily derived from the trees by looking at the areas between the tree edges. These labels exist for the associahedron in any dimension.

Another natural labelling of the pentagon uses elements of the braid group  $B_3$ , which has generators  $\sigma_I$  and  $\sigma_J$  satisfying the group law

$$\sigma_I \sigma_J \sigma_I = \sigma_J \sigma_I \sigma_J. \tag{20}$$

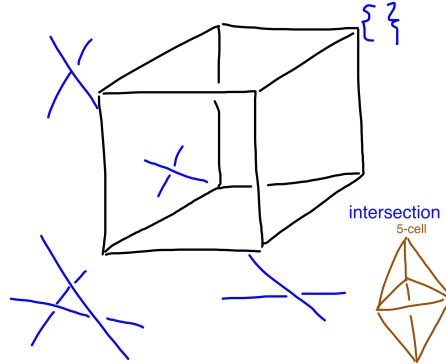


Figure 4: 5-cell from three lines

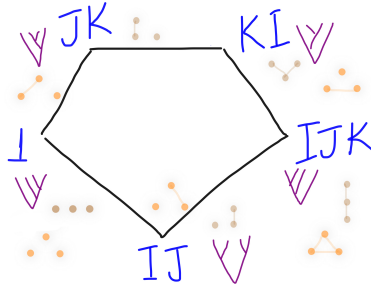


Figure 5: The pentagon vertices as (i) binary rooted trees (purple) (ii) noncommutative forests (brown) (iii) non-crossing partitions (orange)

Observe how the blue words on the pentagon match the non-crossing partitions of the triangle, if the vertices on the triangle are labelled  $I, J, K$ . Now we use the letters  $I, J$  and  $K$  to represent elements of  $B_3$  and include other elements to cover all vertices of the pentagon. A non-crossing partition indexes a braid [62][63] when the partition is assigned a permutation in  $S_3$ , such that the identity 1 is the source of the pentagon, as shown. Given 3 points in a disc, the permutation looks at the triangle defined by the 3 points and says where the braid will send each point around the triangle.

In this way, the braid group  $B_n$  in any dimension is mapped to the vertices of the associahedron in dimension  $n - 1$ , and the generators of  $B_n$  are mapped to initial directions on the polytope.

## 4.2 Fibonacci braids and condensation

An example of a cyclic  $B_3$  representation in  $\mathbb{H}$  is [61]

$$\sigma_{12} = \frac{1}{\sqrt{2}}(1 + i), \quad \sigma_{23} = \frac{1}{\sqrt{2}}(1 + j), \quad \sigma_{13} = \frac{1}{\sqrt{2}}(1 + k). \quad (21)$$

The pentagon also includes the identity 1 and the product  $\sigma_{12}\sigma_{23}\sigma_{13}$ . Under the Pauli matrix representation for  $\mathbb{H}$  we have

$$\sigma_{12}\sigma_{23}\sigma_{13} = \frac{\mathbf{i}}{\sqrt{2}} \begin{pmatrix} 1 & 1 \\ 1 & -1 \end{pmatrix}, \quad (22)$$

which is the Fourier transform. A rotation of this representation in  $SU(2)$  takes us to the Fibonacci anyon representation, which is  $2 \times 2$  for  $B_3$ .

Consider now the closely related  $3 \times 3$  cyclotomic representation of the four strand braid group  $B_4$  in [64], namely

$$\begin{aligned} \sigma_1 &= \begin{pmatrix} e^{3\pi i/5} + \phi e^{-3\pi i/5} & 0 & 0 \\ 0 & e^{3\pi i/5} & 0 \\ 0 & 0 & e^{3\pi i/5} \end{pmatrix}, \\ \sigma_2 &= \begin{pmatrix} e^{3\pi i/5} + \phi^{-1} e^{-3\pi i/5} & 0 & \phi^{-1/2} e^{-3\pi i/5} \\ 0 & e^{3\pi i/5} & 0 \\ \phi^{-1/2} e^{-3\pi i/5} & 0 & e^{3\pi i/5} + e^{-3\pi i/5} \end{pmatrix}, \\ \sigma_3 &= \begin{pmatrix} e^{3\pi i/5} & 0 & 0 \\ 0 & e^{3\pi i/5} + \phi^{-1} e^{-3\pi i/5} & \phi^{-1/2} e^{-3\pi i/5} \\ 0 & \phi^{-1/2} e^{-3\pi i/5} & e^{3\pi i/5} + e^{-3\pi i/5} \end{pmatrix}. \end{aligned} \quad (23)$$

A similar representation exists for all  $B_n$  with  $n \geq 3$  in a dimension given by the corresponding Fibonacci number, and is universal for quantum computation. The qutrit components for the Fibonacci anyon are labeled by the words  $IX$ ,  $XI$  and  $II$ , where  $I$  and  $X$  are the two objects and  $X \otimes X \simeq I + X$  is the non trivial fusion rule. Fibonacci fusion is an example of near-group fusion [65] on a not necessarily invertible object  $X$ , namely

$$X \otimes X \simeq G + kX, \quad (24)$$

for a group  $G$  and ordinal  $k$ . For  $|G| = k + 1$ , the category exists only when  $G$  is the multiplicative part of a finite field, the cyclic group  $C_{p^r-1}$ . Examples of interest include  $(G, k) = (C_2, 1)$ , which has three  $\otimes$  structures [65], and  $(C_{p-1}, p-1)$  for a prime  $p$ , which defines a sequence  $\text{Fib}_p$  of Fibonacci categories, starting at  $p = 2$ . At  $p = 3$  we obtain the rule

$$X \otimes X \simeq I_1 + I_2 + 2X, \quad (25)$$

where we write  $I_1$  and  $I_2$  for the objects in  $G$ . This is known as the  $\mathbf{e}_6/2$  rule. These primes correspond to the qutrit dimension implicit in the discrete cubes, where parity cubes give qubit states. Thus the trit at  $p = 3$  gives a cube whose dimension is fixed by the number of  $X$  letters in a word. For example, the 9 point square holds all words with only one  $X$ , such as  $I_1 X I_1$  at 11 or  $I_2 X$  at 20.

Hopf algebras graded by  $G$  generalise supersymmetry [66], which we see here at  $p = 3$ . Here the object  $I_1 + (I_1 + I_2)$  in the category of vector spaces has a



unique  $C_2$ -graded Hopf structure which is a quotient of  $\mathbb{C}[x, y]$  with antipodes  $S(x) = x$  and  $S(y) = -y$ . The category of  $C_2$  graded vector spaces is thought of as a condensation of the modules for the Hopf structure, which happen to give the category of representations of the permutation group  $S_3$ . Recall that the double  $D(S_3)$  governs electric magnetic duality, as noted below.

The ordinary Fibonacci category  $\text{Fib}_2$  is a condensation of its double category, with special object  $2I + X$  [66]. In this case the antipode satisfies  $S^{10} = 1$ , where

$$S = \mathbf{1}_{I_1} + \mathbf{1}_{I_2} - \frac{\phi^{-1} + \rho i}{2} \mathbf{1}_X, \quad (26)$$

with  $\rho = \sqrt{\phi + 2}$ .

By definition, an algebra object  $A$  in a braided fusion category is *condensable* if (i)  $m\sigma_{UV} = m$  is commutative (ii)  $\text{Hom}(1, A) \simeq \mathbb{F}$  and (iii) the multiplication  $m$  has a splitting map  $A \rightarrow A \otimes A$ . A condensation functor  $\mathcal{C} \rightarrow \mathcal{C}_A$  has a right adjoint, and the composition of adjoints is a Hopf comonad. Thus condensation is the correct setting for the quantisation of classical monads, such as the power set monad for classical logic.

A monad  $T$ , with a structure map  $T^2 \rightarrow T$ , is the ultimate generalisation of an idempotent for measurement. Abstract condensation in some sense concretely encodes the collapse of the wave function. Observe how the Fibonacci fusion rule  $X \otimes X \simeq X \oplus I$  may be interpreted: if tensor is an exponential and  $\oplus$  a product, it behaves as a projective idempotent  $X^2 = IX$ .

For the Fibonacci anyons,  $\phi$  is the quantum dimension of  $X$ . Scaling by the orthogonal  $\rho$ , we obtain both electric and magnetic diagrams, forming dyonic matter at the cosmological mirror. Alternatively, we start with a duality between the 3 point set and the 7 pieces in the intersecting Venn diagram for the subsets of the 3 point set, which are the 7 units of  $\mathbb{O}$  above. Adding antimatter, we get the  $4 + 7 = 11$  dimensions of M theory, within a much larger geometric framework extending to infinite dimensions.

Now we need to consider ribbon representations, starting with the representations of a quantum double. These categories arise with the condensation of anyons to a surface boundary. The Dijkgraaf-Witten model in [7] uses an inner and outer rectangle of plaquettes in a discrete gauge theory for  $G = S_3$ , and an initial Kitaev quantum double Hamiltonian. Here a ribbon is a chain of simplices in the lattice, and each simplex carries a qudit.

The ribbon operators on the lattice form a Hopf algebra dual to  $D(G)$ . Gapped boundary types correspond to subgroups of  $G$ , such as our  $C_3 \subset S_3$ . Recall that  $D(C_3)$  uses the Fourier transform  $F_3$  to make electric magnetic duality manifest [55]. Elementary excitations, by definition [7], are dyonic pairs  $(m, e)$ , where the magnetic charge  $m$  is a conjugacy class for  $G$  and the electric charge  $e$  is an irrep for its centraliser. In other words, a dyon is an irrep for the quantum double. For example,  $m = \{(231), (312)\}$  and  $e = C_3$ . This explains the choice of particle braids in Table 2.

Anyon fusion occurs when two excitations are brought to the same simplex on the lattice. Compare this to figure 7, where two types of overlap triangle are possible. In defects on the boundary, these two options define two distinct tensor

products, and hence a braiding. A gapped boundary in [7] is a condensable algebra object  $\mathcal{A}$ , in a unitary modular tensor category, which is also Lagrangian, meaning that the quantum dimension of  $\mathcal{A}$  is the square root of the full category dimension.

A collection of  $n$  gapped boundaries (internal rectangles) models  $n$  marked points on a Riemann sphere, and hence  $n$  anyons for the fusion trees on the associahedron with  $n$  leaves. A sequence of splittings from the vacuum object, followed by condensation of  $n$  objects to the vacuum, is exactly a choice of two trees on the associahedron, which defines an element of Thompson's  $F$  group, as described in section 3.1. This describes ground state degeneracies in this model. Thus two boundaries  $\mathcal{A}_1$  and  $\mathcal{A}_2$ , along with the vacuum, define a pair of pants diagram, and in this case a bulk anyon particle/antiparticle pair (which condenses) may be represented by a line connecting the two holes on the surface. A ribbon operator for this line is a Wilson line.

Condensation introduces  $3j$  symbols into the structure of the category, for the diagram that first fuses two bulk anyons and then condenses them. The symbols have six indices: three for the  $2 + 1$  bulk anyons and three for the condensation vertices on both this diagram, and the diagram where the two anyons condense straight away. The required axiom is a pentagon with four  $3j$  arrows and one fusion arrow [7], and the commutativity of condensation relates the  $3j$  to the braiding operator. Finally, a  $6j$  symbol is defined across the boundary by a mirror pair of  $3j$  equations, summing over both the input bulk fusion and the mirror fusion index. That is, there are six anyon indices and three condensation indices in total.

Now the Lie algebraic triality automorphism  $\tau$  for  $D_4$  is given by the modular  $S$  and  $T$  matrices for the toric code fusion category, where  $G = S_2$ , as in

$$-2\tau = ((41)(32)) \circ S \circ T = \begin{pmatrix} 0 & 0 & 0 & 1 \\ 0 & 0 & 1 & 0 \\ 0 & 1 & 0 & 0 \\ 1 & 0 & 0 & 0 \end{pmatrix} \begin{pmatrix} 1 & 1 & 1 & 1 \\ 1 & 1 & -1 & -1 \\ 1 & -1 & 1 & -1 \\ 1 & -1 & -1 & 1 \end{pmatrix} \begin{pmatrix} 1 & 0 & 0 & 0 \\ 0 & 1 & 0 & 0 \\ 0 & 0 & 1 & 0 \\ 0 & 0 & 0 & -1 \end{pmatrix}. \quad (27)$$

The 4-basis is  $\{1, e, m, em\}$  [7], and the Lagrangian algebras are  $\mathcal{A}_1 = 1 + e$  and  $\mathcal{A}_2 = 1 + m$ . Condensation sends 1 and  $e$  to 1, and  $m$  and  $em$  to  $m$ . Braiding moves one hole around another.

Consider again the pants diagrams with  $\mathcal{A}_i$  holes, with bulk anyons as lines connecting the circles on the sphere. A pair of  $S^1$  circles is a toric analog of the pair of  $S^2$  which form a 1-handle in a Kirby diagram, which has a link attachment giving a 2-handle [33]. Thus our bulk anyon ribbon is naturally a surface analog of the cancelling 2-handle, and in both cases the  $2 \times 2$  intersection form for the attaching handle is given in (6).

For  $D(C_3)$  we have two condensates:  $1 + e + \bar{e}$  and  $1 + m + \bar{m}$ . This category is the same as  $SU(3)_1 \times \overline{SU(3)}_1$ , which we can represent with two surface layers, so that the bulk line between two holes is categorified to a cylinder handle connecting the holes on different sheets. Sliding tubes around each other in this 3-space reminds us of the spherical category functors used in [33] to define

smooth 4-manifold invariants.

Let us return to the Fibonacci category, which is a condensation of its double. The representation of  $B_n$  in (23) comes with a ribbon twist map  $\theta_X = -e^{\pm\pi i/5}1_X$ . The  $\sqrt{\phi}$  appears as a Lagrangian dimension, and the antipode (26) requires rings with  $\rho$ , as expected.

### 4.3 Templates and ribbons

Categorification is inevitable in quantum computation, where lines are thickened to ribbon strips. These ribbons are used to build surfaces with boundaries. A *template* is a branched surface which includes ribbon vertices, as shown in figures 6 and 7. In 1995, Ghrist [67] showed that there exists a template with four holes containing *all* knots and links, as one would expect for a DNA code.

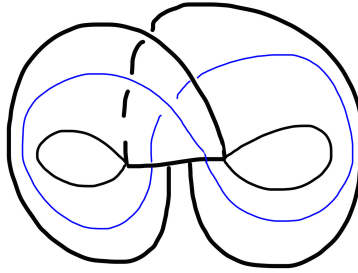


Figure 6: A two-holed Lorenz attractor with blue path

Ribbons may be twisted, and the category has a braiding. Everything happens in either three or six dimensions, because the higher dimensions of M theory just correspond to extra strands in our braid diagrams. This has been discussed elsewhere. Figure 7 illustrates the standard product and coproduct diagrams for a bialgebra, reading the processes down the page. Templates [68] also include up and down tangle ribbon caps, as in the Lorenz template of figure 6. As usual, these exist in categories with duals (see appendix).

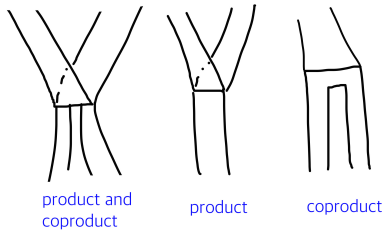


Figure 7: Template vertices

For  $B_3$  diagrams, there exists a universal representation of  $SU(2)$  using the Fibonacci anyons [64][69]. Our Standard Model particle braids [70][58][31][32]

assign  $SU(3)$  color to a choice of one in three twisted ribbon strands. The twist is a  $U(1)$  charge.

A template diagram has a framed link equivalent, as shown in figure 8. The Kirby moves act on framed links as usual.

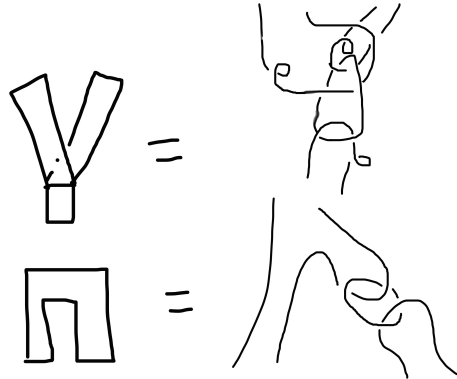


Figure 8: Framed links for template vertices

#### 4.4 Simplices and polytopes

A discrete cube is a cubic piece of the integral lattice with  $d$  points along each edge segment. Its vertex coordinates are noncommutative words in the integer letters. For commutative coordinates, we take diagonal slices. For example, the two words (10) and (01) sit at either end of a diagonal line across the square in the plane. We replace letters with the variables  $X$  and  $Y$ , so that the integers count the number of appearances of  $X$  and  $Y$  in a word. Then  $X$  and  $Y$  are directions in space. For a three letter qutrit alphabet, we get a 2-simplex, as in the examples of figure 9.

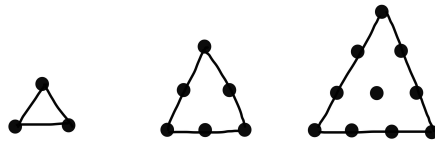


Figure 9: Discrete simplices on three letters

A pentagon has natural integer coordinates [71], as in figure 10, so that three pentagons sit inside the tetractys simplex on the right of figure 9. The corresponding three cubes represent the three mass generations of the Standard Model. Observe the correspondence between these coordinates and words on the pentagon of figure 5. We can do this for the associahedron in every dimension, using discrete simplices with  $d + 1$  points on each edge.

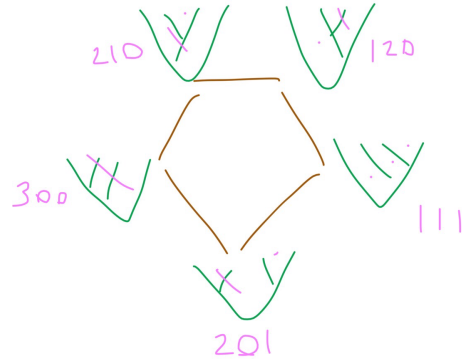


Figure 10: Coordinates for a pentagon

The three dimensional associahedron of figure 13, with 14 vertices, has 24 triangular faces when each of its six pentagons is divided into three triangles. When all faces are triangulated, the associahedron is dual to the 24 vertex permutohedron for  $S_4$ . Coordinates for the associahedron are extended [1] to the 120 vertex polytope of figure 12, which is a pentagon blow up of the permutohedron. Two copies of this polytope catalog the 240 roots of  $\mathfrak{e}_8$ , which are associated to the integral points of the Jordan algebra  $J_3(\mathbb{O})$  [60]. The two copies are scaled by the factors  $(1, \phi)$  in the icosian integers. The scaling  $\rho$  introduces another two copies for the second factor of  $\mathfrak{e}_8$ , putting 16 dimensions into 6 dimensions for gravity. The  $\mathfrak{e}_8$  roots in the magic plane attach Jordan algebra elements to the six points of the star, lying inside the six points of the  $\mathfrak{a}_2$  plane. These are the 12 points of  $\mathfrak{g}_2$  coming from the vertices of the cuboctahedron on the three qutrit cube.

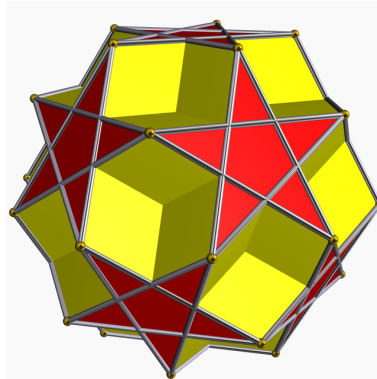


Figure 11: The dodecadodecahedron

The genus 4 dodecadodecahedron of figure 11 has 24 pentagonal faces. As vertices of a permutohedron, 24 points are each blown up into a pentagon on the

120 vertex permutoassociahedron of figure 12. Let us divide the 24 pentagons into two sets, green and red. The green lines connecting the 12 green pentagons form the icosahedron, with 20 triangular faces.

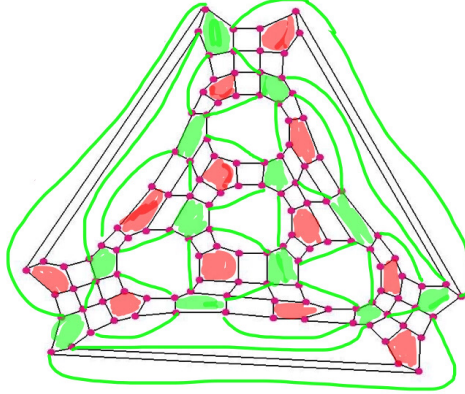


Figure 12: Icosahedron inside the permutoassociahedron

The 12 vertices of the icosahedron have traditional coordinates of the form  $(0, \pm 1, \pm \phi)$ , with cyclic permutations. The 6 lines through a centred pentagon on the icosahedron come from a 6 dimensional lattice. In figure 12, the 8 green triangles inside a 12-gon form a square on 8 out of 20 vertices of the dodecahedron. These are the vertices  $(\pm 1, \pm 1, \pm 1)$ , where the other 12 coordinates are cycles of  $(0, \pm \phi, \pm(\phi - 1))$ . The 12 vertices of the icosahedron are similar to the 12 vertices of the cuboctahedron, inscribed on the 12 edges of a cube.

The golden number  $\rho$  appears in the right angled triangle with an angle of  $36^\circ$  and side lengths  $(\sqrt{5}, 2\rho, \phi\rho)$ . A pentagram component is the right angled triangle  $(1, \sqrt{\phi}, \phi)$ . To include  $1/\sqrt{\phi}$ , as in (23), we need integers of degree 8, or 16 with the complexification of (26). Over  $\mathbb{Z}$ , the  $\mathbf{e}_8$  form then lives in an algebra of 64 dimensions. The cube in dimension  $d$  introduces diagonals of length  $\sqrt{d}$ , starting with the  $\sqrt{2}$  normalisation for qubit operators. We focus on prime dimensions. The surface area of the icosahedron is  $5\sqrt{3}$  and for the dodecahedron it is  $15\phi^2/\rho$ , which introduces  $\rho^{-1}$ .

A discrete direction in our computational space is labelled by the toric paths 1, X, XX, and so on. Given the qudit interpretation, we want an auxilliary space whose directions are given by prime powers, so that all qubit cubes are given by a discrete edge, as in the sides of triangles in figure 9. The figure 9 simplices then belong to higher and higher dimensional qutrit cubes, where the dimension is determined by the number of letters in the word labelling a point. Thus as usual the commutative tetractys diagram gives the 27 points on the 3-cube. The central word XYZ holds 6 permutations for the six paths on the little cube with target point XYZ. But in dimension 4, the 81 path 2-simplex now labels points on a 4-cube. So we can either increase the number of points along an edge in dimension  $p$ , and take the diagonal simplex, or we can fix  $p$

points on an edge and increase the dimension. In the former case, the dimension is constrained by the qudits, and four dimensions carries 4-simplices for 5-dits, while two dimensions carries the qutrits. That is, Langlands geometry is secretly about the 3-dits and 5-dits (and the corresponding cyclotomic fields) that we need to understand the emergence of  $SU(3)$ .

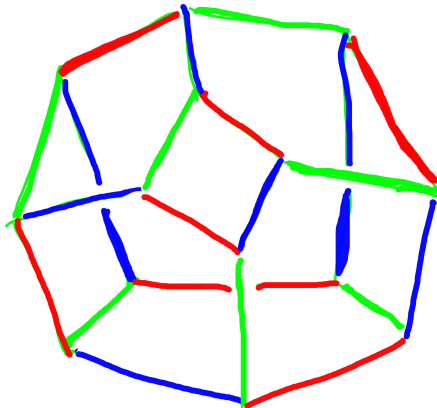


Figure 13: 3-coloring of the associahedron

Introducing the prime 7 in dimension six, we get the cubicuboctahedron and the Mathieu group  $M_{24}$  [72], starting with a permutoassociahedron model for the genus 3 surface. The seven primes (including 1)  $p$  that divide the order of  $M_{24}$  are precisely those such that  $p+1$  is a divisor of 24.  $M_{24}$  has 26 irreps, and their dimensions satisfy nice properties. Only the largest irrep, at dimension 10395, has a new prime factor, namely the 24th prime 83.

## 5 Motivic pairings

Motivically, an integral is a pairing between universal homology and cohomology. The isomorphism between these spaces is natural in a category whose objects have both a geometric and algebraic interpretation. Our topological field theories can become monadic endofunctors. Such a pairing is generically a functor  $F : \mathcal{C}^o \times \mathcal{C} \rightarrow \mathcal{R}$ , so that a map between two such functors  $F$  and  $G$  is a dinatural transformation  $\alpha$  [73], which satisfies the hexagonal rule

$$F(D, C) \rightarrow F(C, C) \xrightarrow{\alpha_C} G(C, C) \rightarrow G(C, D) = \quad (28)$$

$$F(D, C) \rightarrow F(D, D) \xrightarrow{\alpha_D} G(D, D) \rightarrow G(C, D)$$

for every  $f : C \rightarrow D$  in  $\mathcal{C}$ . So it's basically a natural transformation for a span and cospan. Given such a functor  $F$ , a *coend* of  $F$  is a pair  $(C, \alpha)$ , with  $C$  an object and  $\alpha$  a dinatural transformation  $F \rightarrow C$  that maps  $F$  to a constant.

Let  $C$  be a coend in a ribbon category  $\mathcal{C}$ . A *Kirby element* in a ribbon category [74] is a morphism  $f : 1 \rightarrow C$  such that any framed link  $L$  on  $n$  strands defines a good invariant  $T(L, f) = a_L \circ f^{\otimes n}$ , where  $a_L : C^{\otimes n} \rightarrow 1$  is the unique arrow that attaches the link to an object  $X_1 \otimes \cdots \otimes X_n$ . Now the coend of the identity  $1_C$  is a Hopf algebra, say with antipode  $S$  and multiplication  $m : C \otimes C \rightarrow C$ . Then another definition of Kirby element [74] is any  $f : 1 \rightarrow C$  such that  $Sf = f$  and

$$(m \otimes 1_C)(1_C \otimes \Delta)(f \otimes f) = f \otimes f. \quad (29)$$

In a ribbon fusion category, with a finite set  $s$  of simple objects, a coend has the form  $C = \oplus_{i \in s} X_i^* \otimes X_i$ . In the double Fibonacci category  $\text{Fib}_2$ , this gives us the special object  $2I + X$ .

Under the Thompson group construction of section 3.1, a fusion vertex can become a braid crossing on a link. But we can never obtain a 3-coloring by objects, at a vertex, in a Fibonacci category. In a category where we can have three colors at a vertex, like an annihilation  $(e, \bar{e}, 1)$  interaction vertex, the bulk fusions in a ground state  $1 \rightarrow 1$  diagram are removed, and there are no vertices in the resulting link diagram. If the initial crossings lie inside a set of holes on the link diagram, the hole boundaries are then connected by non crossing lines, as for planar algebras. We see then that these holes add structure to the local cutouts used in skein relations.

The moral of the story is that motivic geometry cares about numbers. We do not start with messy real or complex analysis, or classical gauge groups, since these methods rightly exist only as a limit of local (meaning at a prime) computational diagrams. Elsewhere we will discuss the double grading of Khovanov homology, which lives on the smoothing cubes, and also triple gradings for link invariants.

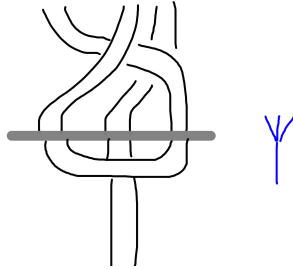


Figure 14: Neutrino braid at mirror with RH line

Figure 14 shows a proper helicity neutrino at a Thompson mirror, with a collapsed mirror braid representing the RH sterile state of the CMB.



## A Number Theory

A good introduction to Number Theory is the book by H. R. Rose (Oxford, 1994). We introduce a selection of interesting fields and rings with a mind to applications in quantum computation and quantum gravity.

By definition, a *number field* extends the rationals by one special real number  $\alpha$ , containing all numbers of the form  $a + b\alpha$  for  $a$  and  $b$  in  $\mathbb{Q}$ . Multiplication and addition in this field  $\mathbb{Q}(\alpha)$  work in the obvious way. Given  $\alpha$ , there is a ring of integers in  $\mathbb{Q}(\alpha)$ , but this is not always the integer multiples of the form  $a + b\alpha$ . For example, when  $\alpha = \sqrt{5}$ , the ring of integers consists of numbers  $a + b\phi$ , where  $\phi = (1 + \sqrt{5})/2$  is the golden ratio.

An *algebraic number* is a root of a finite polynomial with rational coefficients, such that the leading coefficient is 1. The golden ratio is algebraic as a root of  $X^2 - X - 1 = 0$ . Given an algebraic number, there exists a unique such polynomial (of a given degree) with  $\alpha$  as a root. It is useful to factorise the polynomial. Consider the quadratic  $X^2 - k = (X + \sqrt{k})(X - \sqrt{k}) = 0$  of degree 2. The set of roots  $\{+\sqrt{k}, -\sqrt{k}\}$  are called *conjugates* for the field  $\mathbb{Q}(\sqrt{k})$ , and we use this term for polynomials of any degree  $d$ . In terms of the  $d$  conjugates, where  $\alpha = \alpha_1$ , the norm of a number  $\alpha$  is defined by

$$N(\alpha) = \prod_{i=1}^d \alpha_i. \quad (30)$$

Thus  $N(\phi) = \phi \cdot (-1/\phi) = -1$ , while  $X^2 + 3 = 0$  gives  $N(\sqrt{-3}) = 3$ .

Given a set of conjugates for  $\alpha$ , any other element  $\beta$  in  $\mathbb{Q}(\alpha)$  may be written in the form

$$\beta = a_0 + a_1\alpha + a_2\alpha^2 + \cdots + a_{d-1}\alpha^{d-1}, \quad (31)$$

where the  $a_i$  are rational or integer as required. The *field conjugates* of  $\beta$  are the  $d - 1$  numbers of the form  $a_0\alpha_i + \cdots + a_{d-1}\alpha_i^{d-1}$ .

Take a basis  $\{\beta_1, \beta_2, \dots, \beta_d\}$  of  $\mathbb{Q}(\alpha)$ . Typically, we will choose the basis  $\{1, \alpha, \alpha^2, \dots, \alpha^{d-1}\}$ . Now for any  $\mathbb{Q}(\alpha)$ , the basis defines a  $d \times d$  matrix  $M_{ij}$  with columns indexed by the basis and rows by the conjugates of  $\alpha$ . Many examples are given below. The *discriminant* of  $\mathbb{Q}(\alpha)$  is defined by the determinant square  $\Delta = \text{Det}(M)^2$ .

### A.1 Quadratic fields

The degree  $d$  is a quantum dimension, since  $2 \times 2$  matrices ought to be about qubits. When  $\alpha = \sqrt{k}$  for an integer  $k$  with no square factors, the polynomial  $X^2 - k = 0$  defines the field matrix

$$M = \begin{pmatrix} 1 & \sqrt{k} \\ 1 & -\sqrt{k} \end{pmatrix} \quad (32)$$

with discriminant  $\Delta = 4k$ . But for  $\sqrt{-3}$ , the ring of integers has a basis  $\{1, (-1 + \sqrt{-3})/2\}$ , so that  $\Delta = -3$ . Similarly, other negative values of  $k$  give

Table 3: Discriminants for cube roots

$k$	2	3	5	7	11
$ \Delta $	$108 = 27 \times 2^2$	$243 = 27 \times 3^2$	675	1323	3267

negative integral discriminants, in contrast to the positive example of  $\mathbb{Q}(\sqrt{5})$ , which has  $\Delta = 5$  coming from

$$\begin{pmatrix} 1 & \phi \\ 1 & -1/\phi \end{pmatrix}. \quad (33)$$

There are no additional field conjugates in the quadratic case. The opposite sign in  $N(\phi) = -1$ , compared to an ordinary complex norm, is responsible for time in a Lorentzian metric, and  $3 + 5 = 8$  dimensions are associated to the adjoint representation of  $SU(3)$  and octonion algebras.

## A.2 Fields on cube roots

Note that the signs in (33) give the  $2 \times 2$  Hadamard matrix. In dimension 3, we see the qutrit  $3 \times 3$  Fourier transform in the field matrix. Let  $\omega = (-1 + \sqrt{-3})/2$  be the cube root of unity above. For the polynomial  $X^3 - k = 0$  with  $k$  cube free, we have

$$M = \begin{pmatrix} 1 & k^{1/3} & k^{2/3} \\ 1 & \omega k^{1/3} & \bar{\omega} k^{2/3} \\ 1 & \bar{\omega} k^{1/3} & \omega k^{2/3} \end{pmatrix}. \quad (34)$$

Sample discriminants are given in Table 1. Hopefully it is clear that 27 is an important number! This is the determinant square of the Fourier transform, and we have in general  $\Delta = -27k^2$ .

An elliptic curve  $C$  of genus 1 takes the standard form  $Y^2 = X^3 + aX + b$  for rational coefficients, and has a cubic discriminant  $\Delta_C = 4a^3 + 27b^2$ , generalising the example above. If a prime  $p$  divides  $\Delta_C$ , then  $\Delta_C = 0$  in the finite field  $\mathbb{F}_p$ . The finite set of  $\mathbb{F}_p$  solutions to  $C$  defines a Mordell-Weil group for  $C$ , whose order  $N_p(C)$  appears in the zeta function for  $C$ .

## A.3 Fields on fourth roots

When  $\alpha$  is a fourth root, we find that  $\Delta = -k^3$  for  $X^4 - k = 0$ . The matrix is

$$\begin{pmatrix} 1 & k^{1/4} & k^{1/2} & k^{3/4} \\ 1 & ik^{1/4} & -k^{1/2} & -ik^{3/4} \\ 1 & -k^{1/4} & k^{1/2} & -k^{3/4} \\ 1 & -ik^{1/4} & -k^{1/2} & ik^{3/4} \end{pmatrix}. \quad (35)$$

Now let  $\rho = \sqrt{\phi + 2}$  be the diagonal of the golden rectangle. It is algebraic because  $\rho^4 - 5\rho^2 + 5 = 0$ . There are two nice bases for the integers in  $\mathbb{Q}(\rho)$ ,

namely

$$\begin{pmatrix} 1 & \rho & \rho^2 & \rho^3 \\ 1 & -\rho & \rho^2 & -\rho^3 \\ 1 & \sqrt{5} & 5 & 5\sqrt{5} \\ 1 & -\sqrt{5} & 5 & -5\sqrt{5} \end{pmatrix} \text{ and } \begin{pmatrix} 1 & \rho & \phi & \rho\phi \\ 1 & -\rho & \phi & -\rho\phi \\ 1 & \sqrt{5} & 3 & 3\sqrt{5} \\ 1 & -\sqrt{5} & 3 & -3\sqrt{5} \end{pmatrix}, \quad (36)$$

both with  $\Delta = 1055.7281$ . The second basis forms the *golden ring* of integers of the form

$$x_0 + x_1\phi + x_2\rho + x_3\rho\phi \quad (37)$$

for  $x_i \in \mathbb{Z}$ . Note that  $\sqrt{5} = 2\phi - 1$ . In the complex field  $\mathbb{Q}(\rho, i)$ , the ring of integers defines a dense map of  $\mathbb{Z}^8$  into  $\mathbb{C}$ . Alternatively, use the half integer lattice  $\mathbb{Z}^8/2$  (used for  $\mathbf{e}_8$  roots).

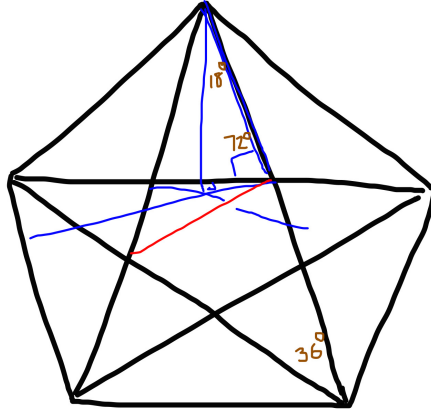


Figure 15: Angle  $36^\circ$  bisection

Figure 14 indicates one of ten possible blue rectangles covering much of the pentagram. The 10 external blue points define a decagon. The chord length on a unit side decagon is  $\rho$ .

#### A.4 Fields on fifth and higher roots

Using the golden phase  $e^{2\pi i/5}$ , the discriminant for  $X^5 - k = 0$  is  $\Delta = 5^5 k^4$ . For example, when  $k = 4$  we have  $\Delta = 800000$ .

We are mostly interested in prime dimensions  $d$  for qudit computation spaces. Let  $\theta$  be the primitive  $d$ -th root of unity. For  $d$  prime, the phase coefficients  $\theta^{ij}$  for  $i, j \in \{0, 1, \dots, d-1\}$  always define the discrete Fourier transform. Then the  $\Delta$  for  $X^p - k = 0$  looks like  $p^p k^{p-1}$ .

#### A.5 Primes and lattices

For quadratic fields, there is a quadratic form that characterises the norm. As expected, the form  $f = aX^2 + bXY + cY^2$  comes with the discriminant

$\Delta_f = b^2 - 4ac$ . In particular, for  $\mathbb{Z}[\omega]$  in  $\mathbb{Q}(\sqrt{-3})$  we have  $\Delta_f = -3$  from  $X^2 + XY + Y^2$ . For  $\mathbb{Z}[\phi]$  the form is  $X^2 + XY - Y^2$  and  $\Delta_f = 5$ . The form  $X^2 + Y^2$  matches the Gaussian integers  $\mathbb{Z}[i]$ . Here  $\mathbb{Q}(\sqrt{5})$  requires  $\phi$  because 5 equals  $+1 \pmod{4}$ . For positive primes  $p \geq 7$  that equal  $3 \pmod{4}$ , such as 7 and 11, the integers have the simple basis  $\{1, \sqrt{p}\}$ , while  $-7 = 1 \pmod{4}$  uses  $(-1 + \sqrt{-7})/2$ .

The Galois primes  $\{2, 3, 5, 7, 11\}$  give the angles for Lie algebra root systems, which satisfy the lattice condition

$$4 \cos^2\left(\frac{2\pi}{p+1}\right) \in \{0, 1, 2, 3\}. \quad (38)$$

Beyond Lie algebras there are other important lattices, notably the Leech lattice in dimension 24 [41].

## B Modular tensor categories

A ribbon category is a braided monoidal category with rigidity, meaning that all objects  $V$  have left and right duals, such that there exist isomorphisms  $\delta_V : V \rightarrow V^{**}$  satisfying [6]

$$\delta_{\mathbf{1}} = 1_{\mathbf{1}}, \quad \delta_{V \otimes W} = \delta_V \otimes \delta_W, \quad \delta_{V^*} = \frac{1}{\delta_V^o}, \quad (39)$$

where  $\delta^o$  is in  $\text{Hom}(V^{***}, V^*)$ . Isomorphisms in the other direction are defined using duals and the flip map, as in

$$\epsilon_V = V^{**} \rightarrow (V \otimes V^*) \otimes V^{**} \rightarrow V \otimes (V^{**} \otimes V^*) \rightarrow V. \quad (40)$$

In any rigid braided monoidal category,

$$\epsilon_{V \otimes W} = \sigma_{WV} \sigma_{VW} (\epsilon_V \otimes \epsilon_W), \quad (41)$$

where  $\sigma$  is the braiding. The ribbon *twist* maps  $\theta_V : V \rightarrow V$  are defined by  $\theta_V = \epsilon_V \delta_V$ . This all implies the balancing axiom,

$$\theta_{V \otimes W} = \sigma_{WV} \sigma_{VW} (\theta_V \otimes \theta_W) \quad (42)$$

and the compatibility condition  $\theta_{V^*} = \theta_V^o$ . Our *semisimple* ribbon categories have a finite set of equivalence classes of non trivial simple objects  $\{V_i\}$  with  $V_0 = \mathbf{1}$  such that  $V_i^*$  is simple and the monoidal structure defines *fusion rules*

$$V_i \otimes V_j = \oplus_k N_{ij}^k V_k. \quad (43)$$

Each  $V_i$  has a quantum dimension  $d_i$ , such that

$$d_i d_j = \sum_k N_{ij}^k d_k. \quad (44)$$

$$s_{ij} = \text{Hopf link with strands } i \text{ and } j$$

$$\text{Twist on strand } i = \frac{s_{ij}}{d_i}$$

For example, the Fibonacci category has two simple objects  $I$  and  $X$  such that  $X \otimes X = I + X$ , and the dimension of  $X$  is  $\phi$  because  $d_X d_X = 1 + d_X$ .

A *modular tensor category* is a semisimple ribbon category with an invertible matrix  $s_{ij}$  defined by the Hopf links for all objects  $V_i$  and  $V_j$ .

Let  $\theta_i$  denote the twist on the simple object  $V_i$ . Define  $p^\pm \equiv \sum_i \theta_i^{\pm 1} d_i^2$ . Then the single unknot denotes  $p^+ p^-$ , and various relations hold between diagrams in the modular tensor category.

$$\text{Twist on strands } i, j = \sum_{ij} \frac{p^+ p^-}{d_i} \text{ (cup and cap diagrams)}$$

A modular tensor category carries a representation of the modular group, generated by diagrams  $S$  and  $T$  and the morphism  $C = \delta_{ij^*} \sigma_{jj}(\theta_j^{-1} \otimes 1)$ , with  $(ST)^3 = \sqrt{p^+/p^-} S^2$  and  $S^2 = C$ .

For any base field, the  $\theta_i$  are roots of unity. In a CFT we have  $\theta_i = e^{2\pi i \Delta_i}$  for the conformal dimension  $\Delta_i$ , and  $(p^+/p^-)^{1/6} = e^{2\pi i c/24}$ , where  $c$  is the central charge. The numbers  $s_{ij}/d_j$  are algebraic integers. For example, in the representation category for the quantum group  $U_q(sl(2))$  this matrix is the  $2 \times 2$  discrete Fourier transform.

**Acknowledgments:** The author thanks Vaughan Jones for speaking about the Thompson group trees in Auckland, some time in 2016.

## References

- [1] M. D. Sheppeard, J. Phys.: Conf. Ser. 1194, 012097, 2019
- [2] M. D. Sheppeard, viXra:1812.0405, 2018
- [3] M. D. Sheppeard, viXra:1712.0076, 2017
- [4] R. Street, *Quantum groups: a path to current algebra*, Cambridge, 2007
- [5] A. Joyal and R. Street, Adv. Math. 102, 1, 20-78, 1993
- [6] B. Bakalov and A. Kirillov Jr, *Lectures on tensor categories and modular functors*, A.M.S., 2001
- [7] I. Cong, M. Cheng and Z. Wang, *Topological quantum computation with gapped boundaries*, arXiv:1609.02037, 2016
- [8] E. Witten, Commun. Math. Phys. 121, 351, 1989
- [9] E. Witten, arXiv:1401.6996, 2014
- [10] E. Witten, talk presented at the conference *Geometry of Quantum Fields and Strings*, University of Auckland, 2020
- [11] V. F. R. Jones, Bull. Amer. Math. Soc. 12, 103, 1985
- [12] M. Khovanov, Duke Math. J. 101, 3, 359-426, 2000
- [13] D. Bar-Natan and S. Morrison, arXiv:math/0606542, 2006
- [14] W. Hsiang, *Lectures on Donaldson theory*, Princeton, 1996
- [15] S. MacLane and I. Moerdijk, *Sheaves and Geometry in Logic*, Springer, 1994
- [16] T. Asselmeyer-Maluga and C. H. Brans, *Exotic smoothness and physics*, World Scientific, 2007
- [17] J. D. Stasheff, Trans. Amer. Math. Soc. 108, 293, 1963
- [18] M. Yoshida, Kyushu J. Math. 50, 493-512, 1996
- [19] A. Gorsky, arXiv:1604.01158, 2016
- [20] S. Gukov, A. Schwarz and C. Vafa, arXiv:hep-th/0412243, 2004
- [21] G. Dungworth, posts at *GalaxyZoo* forums, June 2010
- [22] M. D. Sheppeard, posts at *Arcadian Pseudofunctor*, June 2010
- [23] F. Battaglia and E. Prato, Commun. Math. Phys. 299, 577, 2010
- [24] A. Davydov and T. Booker, arXiv:1103.3537, 2011

- [25] K. Irwin, M. M. Amaral, R. Aschheim and F. Fang, Proc. 4th Int. Conf. on the Nature and Ontology of Spacetime (Varna), p. 117, Minkowski Institute, 2016
- [26] M. Freedman, J. Diff. Geom. 17, 357-454, 1982
- [27] T. Eguchi, H. Ooguri, A. Taormina and S. K. Yang, Nucl. Phys. B 315, 193, 1989
- [28] T. Eguchi, H. Ooguri and Y. Tachikawa, arXiv:1004.0956, 2010
- [29] T. Gannon, arXiv:1211.5531, 2012
- [30] M. C. N. Cheng, J. F. R. Duncan and J. A. Harvey, arXiv:1307.5793, 2013
- [31] C. Furey, Phys. Rev. D 86, 025024, 2012
- [32] C. Furey, Phys. Lett. B 742, 195, 2015
- [33] M. Barenz and J. Barrett, arXiv:1601.03580, 2016
- [34] R. C. Kirby, Invent. Math. 45, 35-56, 1978
- [35] X. L. Qi, R. Li, J.Zang and S. C. Zhang, Science 323, 1184, 2009
- [36] L. Crane and M. D. Sheppeard, arXiv:math.QA/0306440, 2003
- [37] J. C. Baez and J. Vicary, arXiv:1401.3416, 2014
- [38] E. Witten, arXiv:0706.3359, 2007
- [39] M. D. Sheppeard, viXra:1906.0443, 2019
- [40] R. A. Wilson, J. Alg. 322, 2186-2190, 2009
- [41] R. A. Wilson, *The finite simple groups*, Springer, 2009
- [42] M. Rios, private communication, 2018
- [43] M. Kapranov, J. Pure App. Alg. 85, 119, 1993
- [44] J. C. Baez, math.ucr.edu/baez/week102.html, 1997
- [45] J. W. Cannon, W. J. Floyd and W. R. Parry, Enseign. Math. 2, 42, 215-256, 1996
- [46] Y. Inoue, *The four color theorem and Thompson's F and links*, 2016
- [47] A. Heinze and M. Klin, *Loops, Latin squares and strongly regular graphs*, in *Algorithmic algebraic combinatorics and Grobner bases*, eds. M. Klin et al, Springer, 2009
- [48] J. Schwinger, Proc. Nat. Acad. Sci. USA, 46, 570, 1960

- [49] W. K. Wootters and B. D. Fields, *Ann. Phys.*, 191, 363, 1989
- [50] M. Combesure, *J. Math. Phys.* 50, 032104, 2009
- [51] S. H. Ng, A. Schopieray and Y. Wang, arXiv:1812.11234, 2018
- [52] Y. Koide, *Phys. Rev. D* 28, 252, 1983
- [53] Y. Koide, *Phys. Lett. B* 120, 161, 1983
- [54] C. A. Brannen, *The lepton masses*, <http://www.brannenworks.com>, 2006; various papers at viXra
- [55] M. D. Sheppeard, viXra:1709.0035, 2017
- [56] J. Fuchs, C. Schweigert and C. Stigner, arXiv:1007.0401, 2010
- [57] P. T. Johnstone, *Stone spaces*, Cambridge, 1982
- [58] M. D. Sheppeard, *Gluon phenomenology and a linear topos*, PhD thesis, University of Canterbury, 2007
- [59] M. D. Sheppeard, viXra:1908.0481, 2019
- [60] P. Truini, M. Rios and A. Marrani, arXiv:1711.07881, 2017
- [61] L. H. Kauffman, arXiv:1710.04650, 2017
- [62] E. L. Chisholm and J. McCammond, *Braid groups and Euclidean simplices*, 2015
- [63] J. McCammond and R. Sulway, *Artin groups of Euclidean type*, 2017
- [64] L. H. Kauffman and S. L. Lomonaco Jr, arXiv:0804.4304, 2008
- [65] J. Siehler, *Alg. and Geom. Top.* 3, 719-775, 2003
- [66] S. X. Cui, M. S. Zini and Z. Wang, arXiv:1809.00245, 2018
- [67] R. W. Ghrist, *Elec. Res. Announcements of the A.M.S.*, 1, 2, 91, 1995
- [68] L. H. Kauffman, M. Saito and M. C. Sullivan, *Quantum invariants of templates*, 2001
- [69] B. Field and T. Simula, arXiv:1802.06176, 2018
- [70] S. O. Bilson-Thompson, arXiv:hep-ph/0503213, 2005
- [71] A. Postnikov, *Int. Math. Res. Not.* 2009, 1026, 2009
- [72] D. Richter, <http://homepages.wmich.edu/~drichter/mathieu.htm>
- [73] S. MacLane, *Categories for the working mathematician*, Springer, 2000
- [74] A. Virelizier, *Quantum invariants of 3-manifolds, TQFTs and Hopf monads*, Habilitation, Univ. Montpellier 2, 2010